Development 111, 909–920 (1991)
Printed in Great Britain © The Company of Biologists Limited 1991

Retarded nuclear migration in *Drosophila* embryos with aberrant F-actin reorganization caused by maternal mutations and by cytochalasin treatment

KO HATANAKA* and MASUKICHI OKADA†

Institute of Biological Sciences, The University of Tsukuba, Tsukuba, Ibaraki 305, Japan

* Present address: Department of Pharmacology, School of Medicine, Kitasato University, Sagamihara, Kanagawa 228, Japan
† Author for correspondence

Summary

Three X-linked mutations of *Drosophila melanogaster*, *gs(1)N26*, *gs(1)N441* and *paralog*, had a common maternal-effect phenotype. Mutant embryos show reduced egg contraction that normally occurs at an early cleavage stage in wild-type embryos. In addition, the mutants exhibited retarded nuclear migration while synchronous nuclear divisions were unaffected. The retarded migration causes nuclei to remain in the anterior part of the embryo retaining their spherical distribution even in a late cleavage stage. This consequently results in an extreme delay in nuclear arrival in the posterior periplasm. A mutant phenocopy was induced in wild-type embryos that were treated with cytochalasin B or D at a very early cleavage stage. Remarkable differences were noticed in the organization of cortical F-actin between the mutants and the wild type throughout the cleavage stage: obvious F-actin aggregates were dispersed in the cortex of mutant embryos, in contrast to the wild type where the cortical F-actin layer was smooth and underlying F-actin aggregates were smaller than those in the mutants; the transition of the distribution pattern of F-actin in the yolk mass, from the centralized to the fragmented type, occurred later in the mutants than in wild type. The results suggest that these mutations affect the mechanism underlying establishment and transition of F-actin organization required for normal egg contraction and nuclear migration in the cleavage embryos.

Key words: *Drosophila*, cleavage embryo, mutant, nuclear migration, F-actin, cytochalasin, phenocopy.

Introduction

In *Drosophila* embryos, cleavage nuclei migrate away from each other to approach the egg surface during the first eight synchronous intravitelline mitoses. At the completion of the 8th mitosis (256-nucleus stage or cycle 9, Foe and Alberts, 1983), nuclei have reached subcortical cytoplasm in the somatic region while they have penetrated the cortex or periplasm at the posterior pole region, where the nuclei are to contribute to pole cell formation. After the 9th division, about 350 nuclei penetrate the periplasm in the somatic region. Nuclei divide four more times in the periplasm, and then the plasma membrane infolds to isolate every syncytial blastoderm nucleus into a blastodermal cell.

Cytological studies on early *Drosophila* embryos have shown that the distribution pattern of cytoskeletal elements is characteristic of the stage and the area of embryos (Warn and Magrath, 1983; Warn *et al.* 1984; Warn *et al.* 1985; Miller *et al.* 1985; Warn, 1986; Warn and Warn, 1986; Karr and Alberts, 1986). It has accordingly been suggested that the cytoskeletal elements play key roles in some critical events in the early development, such as nuclear penetration of periplasm, nuclear cap formation, pole cell formation and blastodermal cell formation. However, the studies have not been extended to the mechanism of nuclear migration at stages earlier than cycle 8.

Many maternal-effect mutations affecting early development of *Drosophila* embryos have been isolated (Gans *et al.* 1975; Mohler, 1977). The phenotypes of these mutants were reported to include the cessation of development due to failure of various important processes, for example fertilization, nuclear division, blastoderm formation, or gastrulation (Zalokar *et al.* 1975). Some other maternal-effect mutants were characterized as grandchildless due to their lack of pole cell and consequent germ cell formation (Thierry-Mieg, 1976; Niki and Okada, 1981; Thierry-Mieg, 1982). Although detailed cytological analyses have been made in a maternal-effect mutant *giant nuclei* (Freeman *et al.* 1986) and in several zygotic mutants (Wieschaus and

Sweeton, 1988; Merrill *et al.* 1988), most of the maternal-effect mutants affecting cleavage-stage embryos have not been cytologically analysed in detail. Elucidation of spatiotemporal changes in the cytoskeletal organization in mutants with disordered cleavage and nuclear migration will shed light on the structure of the machinery that drives nuclei outwards during the cleavage stage.

We have chosen three maternal-effect mutations, *gs(1)N26*, *gs(1)N441* and *paralog* (abbreviated as *N26*, *N441* and *par*, respectively). Although *N26* and *N441* were originally isolated as grandchildless-class mutations (Niki and Okada, 1981), *N26* has been reported to have an abnormal pattern of nuclear arrival in the periplasm (Niki, 1984), and our preliminary observation showed that *N441* initiated its abnormality in the nuclear migration at an early cleavage stage. *par* was isolated as a female-sterile mutant (Gans *et al.* 1975), and its dirorder in blastoderm formation was reported afterwards (Zalokar *et al.* 1975). Here we report that each of the three mutations at different loci affects both F-actin organization and nuclear migration in the cleavage stage.

Materials and methods

Fly stocks

Oregon-R was used as a wild-type strain. *N26* and *N441* (Niki and Okada, 1981) were maintained heterozygous for the FM7 balancer. A *y par v*/FM3 stock was kindly provided by Dr M. Masson (CNRS). The *par* mutant was isolated and named X^{1122} by Gans *et al.* (1975), its phenotype in blastoderm formation was described by Zalokar *et al.* (1975), and its genetic analysis was made by Thierry-Mieg (1982). The three mutations that we used for the present work were confirmed to complement completely with each other (data not shown).

For cytological mapping of *N26* and *N441*, the strains with deficiency around expected genetic loci as described in Lindsley and Zimm (1987) were used. The strains used in this work were provided by Pasadena Stock Center, California State University, National Institute of Genetics (Mishima) and Dr Y. Hotta (University of Tokyo). hfs^{EH326} used for the complementation test with *N26* was provided by Dr D. F. Eberl. All stocks were maintained at 25°C on a dead yeast–corn meal–glucose–agar or dead yeast–corn meal–sucrose–agar medium.

Egg collection

Newly emerged homozygous mutant females were fed for 4–5 days at 25.5±1.0°C (restrictive temperature), or for 8–10 days at 18.0±1.0°C (permissive temperature) before being allowed to lay eggs. Since all the mutations that we analysed have temperature-sensitive periods during oogenesis (Niki and Okada, 1981; Thierry-Mieg, 1982; Maruo and Okada, 1984), eggs collected from these females were produced entirely under either the restrictive condition or the permissive condition.

To collect wild-type eggs to be subjected to an inhibitor treatment, female flies were allowed to lay eggs on an agar plate for 20 min at 25°C, after a first 90 min egg collection was discarded.

Nuclear staining

Nuclear staining in whole-mount embryos was performed basically according to Zalokar and Erk (1977). Embryos were manually dechorionated, fixed, hydrolysed in 3 N HCl for 12 min at 55°C, and stained with basic fuchsin. The embryos were then rapidly washed on a Teflon-coated depression slide (the Teflon spray was purchased from IUCHI), with 70% ethanol and dehydrated through an ethanol series (70–100%), infiltrated with *n*-butanol and xylene for 5 min each, and whole-mounted in Eukitt (O. Kindler, Germany).

Application of inhibitors

Appropriately staged embryos were manually dechorionated, transferred on a siliconized depression slide, permeabilized with octane for 20 s and incubated in a drop of an incubation medium containing a given concentration (up to 10 $\mu g\,ml^{-1}$) of cytoskeletal inhibitors for 5 min (Limbourg and Zalokar, 1973). After the medium was removed, the embryos were covered with a drop of paraffin oil. The slide was kept in moist air at 25°C to allow the embryos to develop to the required stage. After incubation, embryos were briefly washed with heptane three times, fixed and stained according to Zalokar and Erk (1977), and whole-mounted in Eukitt. Because it was difficult to remove the vitelline membrane in colchicine-treated embryos by the above methods, these embryos were fixed with 8% paraformaldehyde in 10 mM PBS (pH 7.2) for 5 min and the vitelline membrane was removed in the same fixative on double-stick tape (Scotch), followed by postfixation in the same fixative for 30 min and staining with 0.5 $\mu g\,ml^{-1}$ DAPI for 10 min. The embryos were washed, whole-mounted in glycerol and observed with an epifluorescence microscope (Nikon).

Cytochalasin B and D, colchicine and lumicolchicine were purchased from Sigma. Cytochalasin was dissolved in dimethylsulfoxide (DMSO, 1 $mg\,ml^{-1}$) and this stock solution was diluted to make a working solution, in which the concentration of DMSO was less than 1%, and embryos developed normally (Zalokar and Erk, 1976; our present observations).

Double fluorescent staining

Manually dechorionated embryos were fixed with 8% paraformaldehyde in 10 mM PBS (pH 7.2) according to Warn and Magrath (1983). Embryos were punctured at the dorsal side in the fixative solution with a fine glass needle on a micromanipulator to facilitate the entry of fixative into the embryos. Double-staining with rhodaminyl phalloidin (Molecular Probes Inc.) and DAPI (Sigma) was performed according to Warn *et al.* (1984). Because F-actin was found to become extremely sensitive to fixation if embryos were overdesiccated, embryos were kept in moist air using an ultrasonic humidifier during dechorionation, which took approximately 10 min. It was also necessary to determine an optimum desiccation time for each strain to prevent cytoplasm from leaking out of the puncture. The optimum desiccation time varied from 1.5 min (*par*) to 3.5 min (wild type).

For frozen sections, embryos were fixed, stained and washed, infiltrated with 50% Tissue-Tek II (MILES) for 5 min, embedded in Tissue-Tek II, oriented with a hand-driven centrifuge, and frozen in isopropanol cooled with liquid nitrogen. 5 μm serial frozen sections were made, rapidly dried on a glass slide, and mounted in Tissue-Tek II just before observation.

As a control, embryos were stained only with DAPI, or were pretreated with 1 $mg\,ml^{-1}$ phalloidin (Sigma) in 10 mM PBS (pH 7.2) for 15 min to block the specific binding of rhodaminyl phalloidin. Neither autofluorescence nor non-specific binding of the fluorescent dye was detectable.

Preparations were observed with an epifluorescence microscope (Nikon) or a laser scanning confocal fluorescence microscope, MRC-500 (Bio-Rad Inc.), and photographed on Panatomic-X or Ektachrome 100 film (Kodak).

Results

Egg contraction

Deficiency in egg contraction was the first abnormality recognized in the development of *N26*, *N441* and *par* embryos that had been derived from their respective homozygous mothers. In the wild type, ooplasm contracts during the early cleavage stage resulting in a space under the vitelline membrane at the posterior pole region (Fig. 1A). So-called pole buds protrude into this space to form pole cells. In contrast, mutant embryos had hardly any space under the vitelline membrane throughout the cleavage stage, provided that the embryos were derived from homozygous females raised at a restrictive temperature (Fig. 1B–D).

Division and migration of nuclei

Nuclear arrival in the posterior pole periplasm has been reported in *N26* to be delaying by 30 min compared with nuclear arrival in the other regions (Okada, 1982). Observations with a time-lapse video confirmed this and revealed a similar delay in *N441* and *par*.

This delay could be caused either by an elongated mitotic cycle in the posterior half of the embryo, or by retarded nuclear migration toward the posterior. To test these hypotheses, we observed more than a hundred fixed cleavage embryos of each strain and recorded the number, the distribution pattern and the mitotic phase of nuclei in every single embryo.

The number of nuclei was found to increase by a factor of two even in mutant embryos, independently of the temperature conditions in which their mothers were raised. However, the distribution pattern of nuclei was different between the mutant and wild-type embryos.

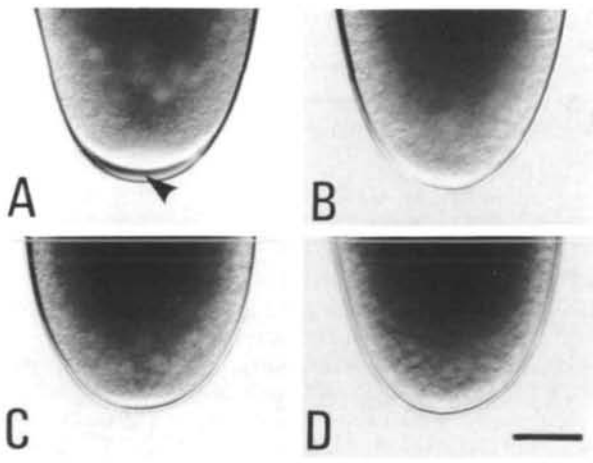

Fig. 1. Posterior pole region of live cleavage embryos photographed with Nomarski optics. Wild-type (A), *N441* (B), *N26* (C) and *par* (D) embryos are shown. Arrowhead indicates the space between egg plasma membrane and vitelline membrane. Bar represents 50 μm.

The difference was most conspicuous at late cleavage stages (Fig. 2B–D). In wild-type embryos at cycle 8 (128-nucleus stage; Foe and Alberts, 1983), nuclei were distributed equidistance from the cortex and from each other causing the nuclei to line up on the subcortical plane (Fig. 2A). In cycle-8 mutant embryos, however, nuclei (except those destined for yolk nuclei) have migrated an approximately equal distance from their original position, where karyogamy occurred, resulting in a somewhat off-spherical nuclear distribution (Fig. 2B–D). This indicates that posteriorward and anteriorward migration of nuclei is affected by the mutations. The tardy posteriorward nuclear migration frequently caused failure in pole cell formation (Okada, 1982), and also disorder in segmentation.

The mitotic cycle of cleavage nuclei was almost completely synchronized even in mutant embryos at cycle 6. At cycle 7 through 9, a mitotic wave, in which a shift in mitotic phase never exceeded one mitotic cycle, was observed in mutant embryos. It occurred most frequently in embryos with weak phenotype, occasionally produced by homozygous mutant females raised under permissive conditions (Fig. 3A). This weak mitotic wave drifted always from posterior to anterior, parallel to the anteroposterior axis and also to the gradient of local nuclear density. In mutant embryos deriving from homozygous females raised under a restrictive condition, prominent cortical mitotic waves were constantly observed throughout the syncytial blastoderm stage (Fig. 3B).

On the other hand, weak mitotic waves starting from both poles and colliding in the middle region of an embryo were observed even in wild-type embryos at the syncytial blastoderm stage. The direction of a mitotic wave was consistent with the gradient of local nuclear density in wild-type as well as in mutant embryos. It may be a general rule that the lower the local nuclear density the faster a mitotic cycle proceeds in a syncytium.

In wild-type embryos, nuclei penetrate the cortex in the posterior pole region at cycle 9, and in other regions at cycle 10. In mutant embryos, however, nuclei prematurely penetrated the cortex in a region around 70% egg length (posterior pole as 0% egg length) at cycle 8 or 9 (Fig. 2C,D).

Phenocopy induction by treatment of wild-type embryos with cytochalasins

Treatment of a wild-type embryo at or before cycle 3 with 1–10 $\mu g\,ml^{-1}$ cytochalasin B or 0.5–10 $\mu g\,ml^{-1}$ cytochalasin D for 5 min caused the embryo to exhibit the mutant type nuclear distribution (Fig. 4B). When treated at a later stage (cycle 4–6) or when cycle 3 embryos were treated with a slightly lower concentration of cytochalasins, embryos showed a delay in nuclear migration toward both poles. This confirmed the report by Zalokar and Erk (1976). The treatment with cytochalasin at a concentration of 0.01 $\mu g\,ml^{-1}$ or less had no visible effect on nuclear migration, and normal larvae hatched from the treated embryos. These results suggest that the three mutants studied here may

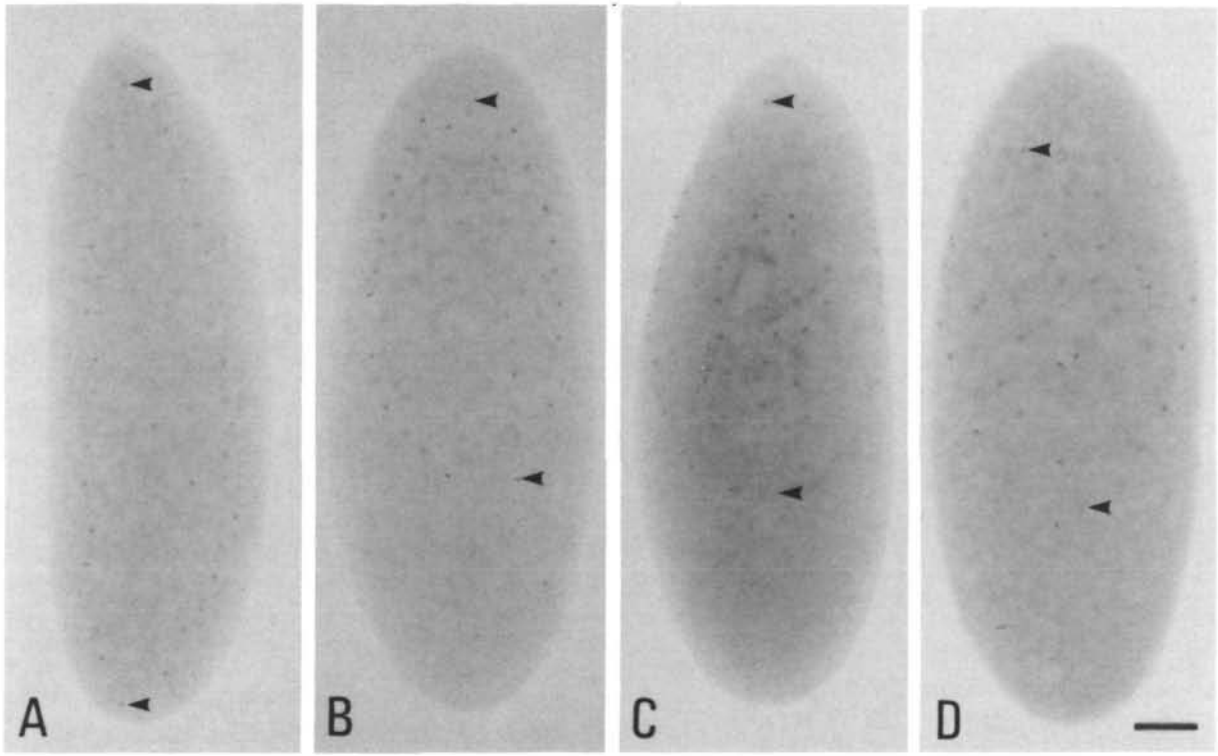

Fig. 2. Whole-mount embryos at cycle 8. Nuclei were stained with basic fuchsin. Wild-type (A), *N441* (B), *N26* (C) and *par* (D) embryos are shown. Anterior pole to the top. Arrowheads indicate the most anterior and the most posterior nucleus in each embryo. Bar represents 50 μm.

have genetically caused defects in a microfilament system that is involved in the machinery working at early cleavage stages for the migration of nuclei toward the poles.

Colchicine had a quite different effect on nuclear migration. Treatment of wild-type embryos before cycle 4 with 0.1–0.5 $\mu g\,ml^{-1}$ colchicine for 5 min did not alter cleavage mitotic cycles and scarcely hindered the migration of nuclei toward both poles. However, nuclear migration towards the lateral cortex was heavily inhibited. As a result, colchicine results in the nuclei in cycle-7 embryos being distributed in an extremely elongated ellipsoidal region (Fig. 4C). This is completely different from the mutant phenotypes. A treatment with 0.01 $\mu g\,ml^{-1}$ colchicine or 10 $\mu g\,ml^{-1}$ lumicolchicine had no visible effect on nuclear migration. It can thus be concluded that the three mutations here described have no effect on the microtubule system in cleavage embryos.

F-actin distribution in wild-type embryos

To determine whether the abnormal nuclear migration in mutant embryos is caused by defects in the microfilament system, we compared wild-type embryos with mutant embryos for the distribution of F-actin during the cleavage stage, using rhodaminyl phalloidin as an F-actin-specific probe.

In wild-type cleavage embryos and unfertilized eggs, F-actin was densely distributed throughout the cortex. The cortical F-actin layer was relatively uniform with numerous microprocesses on the outer surface, and very small F-actin aggregates were observed lining the inner surface of the smooth cortical F-actin layer throughout the cleavage stage (for example, see Fig. 5C) as previously reported (Warn, 1986; Karr and Alberts, 1986).

Since the strong fluorescence from the cortex interferes with the observation of weak fluorescence from the inside of whole-mount specimens, cryostat sections of specimens were observed for detecting F-actin localized deep in the yolk. A laser confocal microscope has been found to be more reliable for the observation of the deeply localized F-actin. In addition, it was effective in disclosing a loose 30 μm-thick F-actin-enriched layer (Fig. 5K, between arrows) lining the cortical F-actin layer.

The F-actin distribution pattern in the yolk mass changed with development. At cycle 2 (2-nucleus stage), a very weak signal of F-actin was recognizable midway between two nuclei (Fig. 5A), while no other stable F-actin signal was detected except in the cortex. In unfertilized eggs and cycle-1 embryos, no F-actin signal was detectable in the yolk, suggesting that it was formed during or shortly after the first mitosis. The F-actin signal persisted up to cycle 4 at the geometrical center of a 'nuclear sphere', a virtual sphere on which cleavage nuclei are distributed (Fig. 5C,D). Confocal images showed several small aggregates of F-actin in this region (Fig. 5K, arrowheads). We refer to this accumulation of F-actin at the center of the nuclear sphere as a central domain of F-actin. The central

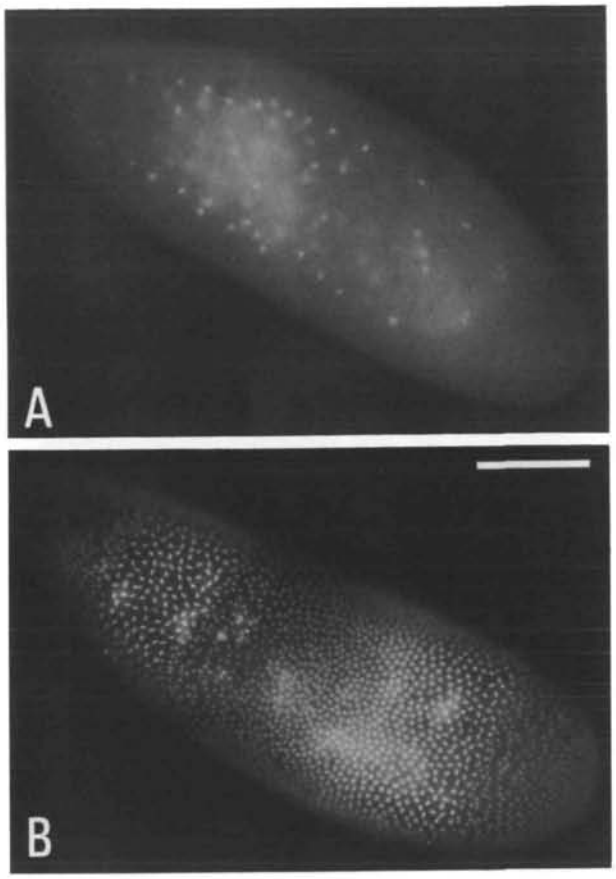

Fig. 3. Mitotic waves in *N441* embryos. (A) A cycle-8 embryo from a mother raised under a permissive condition (note that the nuclei close to the posterior pole are in anaphase to telophase in advance); (B) a syncytial blastoderm embryo from a female raised under a restrictive condition. Nuclei were stained with DAPI. Anterior pole to the top-left corner. Bar represents 100 μm.

domain continued to grow during cycle 2 through 4 becoming more easily detectable, although it was much weaker than cortical F-actin even at cycle 4.

At cycle 5 (16-nucleus stage), the pattern of F-actin distribution in the yolk mass was variable among embryos. In some embryos, the central domain of F-actin was weaker than that of cycle-3 or -4 embryos, was elongated anteroposteriorly and was subdivided into several fragments, all of which avoided nuclei (Fig. 5E). In the other embryos, the central domain became very weak and hardly detectable while the very weak signal of F-actin was often detectable in energids (data not shown); this F-actin domain will be referred to as the energid domain. As soon as the energid domains appeared, the central domain rapidly declined and disappeared, and the central domain was no longer detectable at cycle 6. From these observations, we conclude that the transition of F-actin distribution from the central to the energid domain takes place at cycle 5 in wild-type embryos.

At cycle 6 through 9, energid domains of F-actin were observed as areas of generally brighter phalloidin staining with many small aggregates (Fig. 5G,I). A strong staining of the nuclear islands with rhodaminyl phalloidin at cycle 9 was also shown by Warn (1986). When the nuclei in energids were in metaphase to anaphase, energid domains of F-actin were all dumb-bell-shaped with their long axis in accordance with the axis of the mitotic spindles (Fig. 5G–J).

After nuclear arrival in the cortex, or after the energid domains had anastomosed with the cortex, the

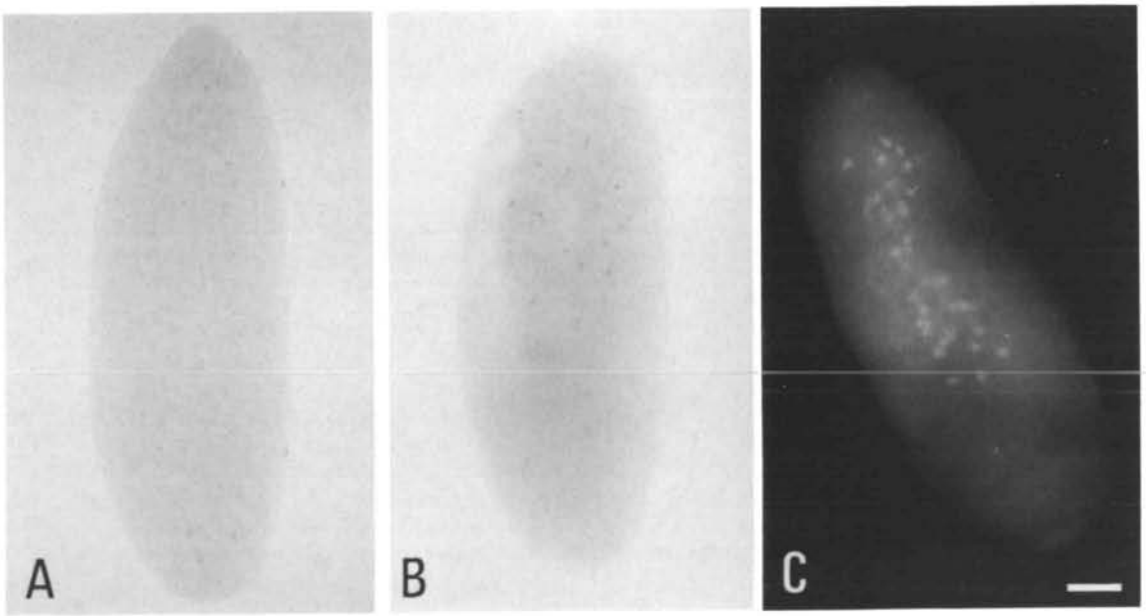

Fig. 4. Effects of cytoskeletal inhibitors on nuclear migration. (A) An untreated wild-type embryo at cycle 7; (B) a cycle-7 wild-type embryo treated with 1 μg ml^{-1} cytochalasin B for 5 min at cycle 2; (C) a cycle-7 wild-type embryo treated with 0.2 μg ml^{-1} colchicine for 5 min at cycle 2. Nuclei were stained with basic fuchsin (A and B), or with DAPI (C). Anterior pole to the top. Bar represents 50 μm.

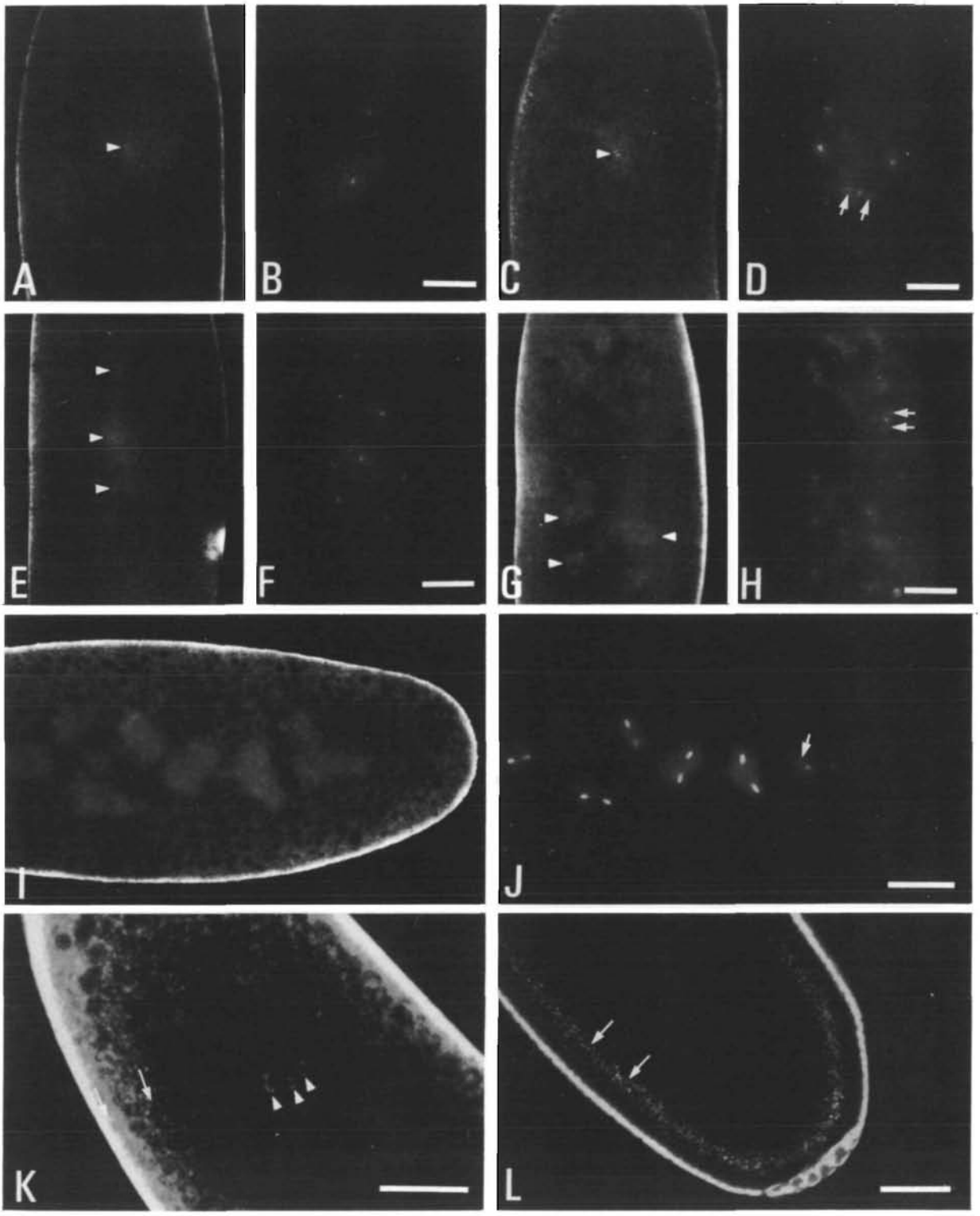

distribution of cortical F-actin was no longer uniform but showed a periodical pattern corresponding to the distribution of nuclei. These observations confirmed the previous reports (Warn *et al.* 1984; Warn *et al.* 1985; Warn, 1986). In addition, a deeper layer of F-actin aggregates surrounding the contracting central yolk mass appeared at cycle 10 and persisted through the syncytial blastoderm stage (Fig. 5L arrows).

F-actin distribution in mutant embryos and phenocopies

During the early cleavage stage, mutant embryos had many F-actin aggregates scattered in the cortical F-actin layer (Fig. 6B–D,F–H). Although small F-actin aggregates were abundant immediately beneath the cortical F-actin layer in wild-type embryos, as mentioned above, the aggregates in the mutants were significantly

Fig. 5. The distribution of F-actin in wild-type embryos. Embryos were stained with rhodaminyl phalloidin (A, C, E, G, I, K and L), or with DAPI (B, D, F, H and J). (A and B) The same cycle-2 embryo; (C and D) the same cycle-3 embryo; (E and F) the same cycle-5 embryo; (G and H) the same cycle-6 embryo; (I and J) the middle and posterior region of the same cycle-6 embryo. (K) The anterior region of a cycle-3 embryo; (L) the posterior region of a cycle-11 embryo. (A–H) Whole-mounted embryos; (I and J) frozen-sections; (K and L) confocal images of whole-mounted embryos. Anterior poles are to the top (A–H), to the left (I and J), or to the top-left corner (K and L). Arrowheads in A, C, E and K indicate the central domain of F-actin; in G indicate energid domains of F-actin. A 30 μm-thick F-actin-enriched layer is indicated between arrows in K. Arrows in L indicate a deeper layer of F-actin surrounding the central yolk mass. A bright spot in E is artifact. In the wild-type strain that we used, fine granules that bind to DAPI are found in cytoplasm surrounding nuclei and at poles of mitotic spindles (arrows in D, H and J). Bars represent 50 μm.

larger in size with a maximum diameter of 5 μm and smaller in number, and they were rather irregular in shape (Fig. 6F, arrowheads). The density of these aggregates in the mutants was variable between embryos or even between regions in a single embryo. They were most remarkable in *N26* among the three mutants. These aggregates were not detectable during oogenesis in any of the mutants that we studied. In embryos derived from mutant females raised under a permissive condition or from heterozygous females, the cortical F-actin layer was indistinguishable from that in wild-type embryos.

F-actin aggregates in the cortex were still prominent at cycle 6 and they gradually disappeared afterwards. The disappearance of the aggregates was initiated in the area at around 70 % egg length level (the posterior pole as 0 %), where nuclei prematurely penetrate the cortex in mutant embryos at cycle 8–9. Then the area without the aggregates widened toward the poles (Fig. 7A). At around cycle 12, when the whole cortex of mutant embryos was loaded with nuclei, the cortex restored its normal-type, smooth distribution of F-actin, although the mitotic waves drifting from posterior to anterior, which are characteristic of the mutants, were still prominent at this stage (Fig. 7C,D). Probably the effects of mutations on the organization of cortical F-actin is limited to the cleavage stage.

At cycle 2, the central domain of F-actin was perceivable only on rare occasions in mutant embryos. At or after cycle 3 the central domain were clearly observable, and it is gradually enlarged with development (Fig. 8A,C,E,G–I). The transition of F-actin distribution from the central to the energid domain started at cycle 7 and proceeded slowly. It is apparently later in the mutants than in the wild type (Fig. 8J). In addition, the loose F-actin-enriched layer lining the cortical F-actin in the mutants was about 5 to 10 μm thick (Fig. 8G–I) and was generally less developed than the 30 μm thick layer in wild-type embryos.

In a phenocopy induced by treating wild-type

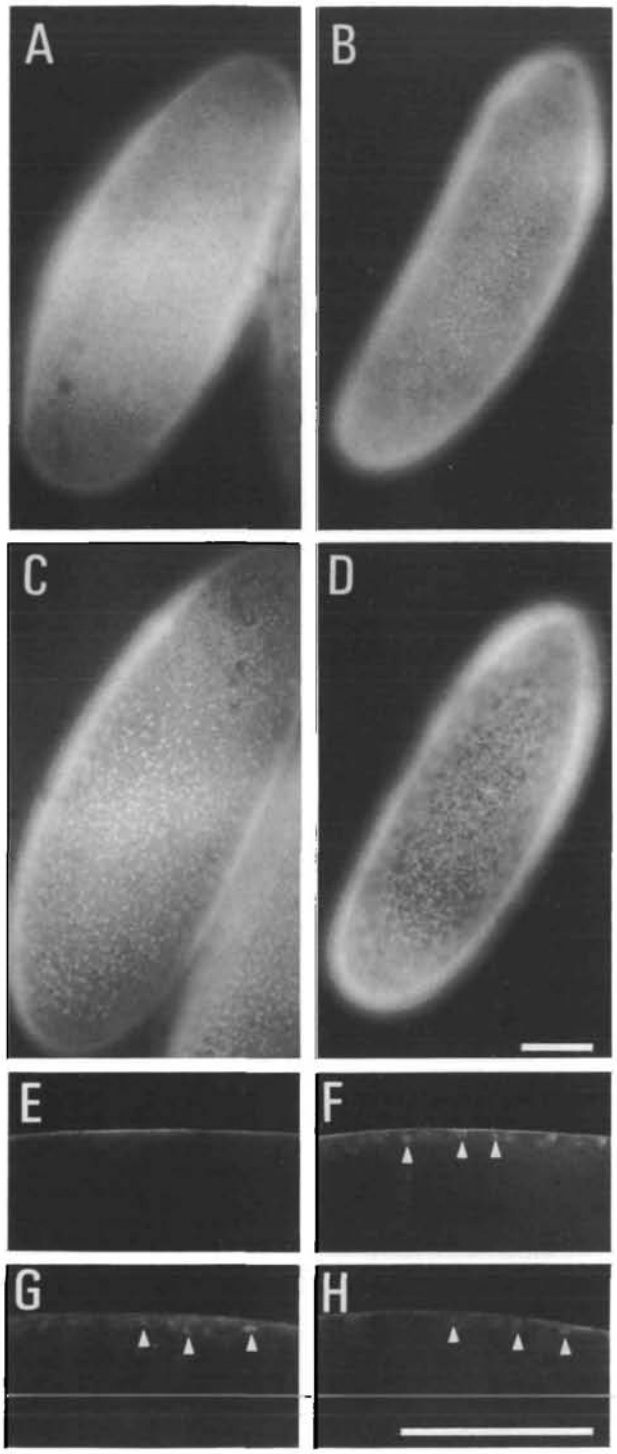

Fig. 6. Cortical F-actin in cleavage embryos. Embryos were stained with rhodaminyl phalloidin. Wild-type (A and E). *N441* (B and F), *N26* (C and G) and *par* (D and H) embryos are shown. Focus is on the surface of embryos in A–D, and on the margin of whole-mounted embryos in E–H, in which arrowheads indicate mutant-type cortical F-actin aggregates. Anterior poles are to the top-right corner in A–D. Bar represents 100 μm.

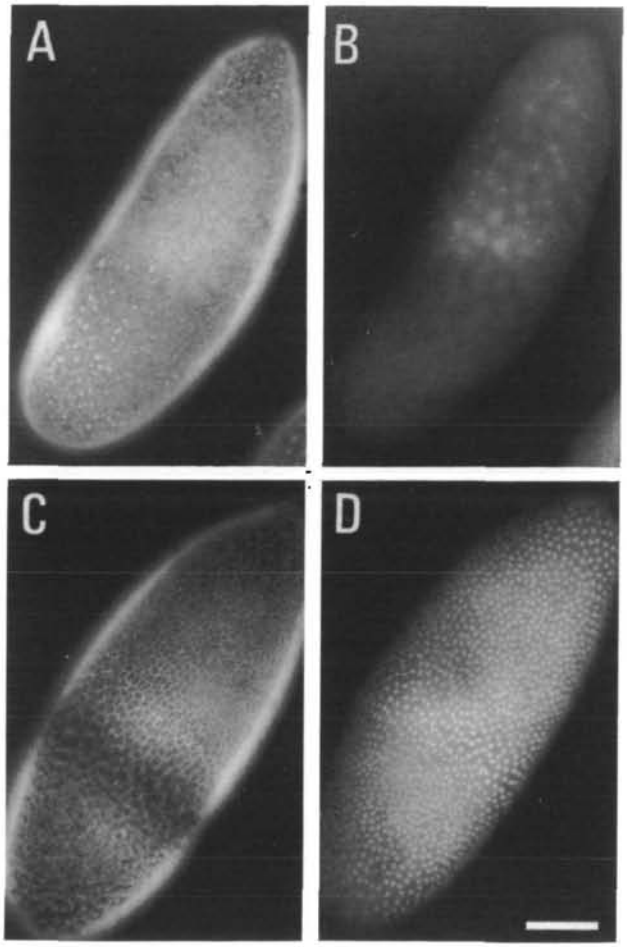

Fig. 7. Normal cortical F-actin organization restored to mutant embryos after nuclear arrival in the cortex. Rhodaminyl–phalloidin stained *N26* embryos at cycle 9 (A) and at late syncytial blastoderm stage (C) showing cortical F-actin; nuclei of the same embryos shown in A and C are visualized by DAPI staining in B and D respectively. Focus is slightly deeper in B than in A. Anterior poles are to the top-right corner. Bar represents 100 μm.

embryos with 1 $\mu g\,ml^{-1}$ cytochalasin B, the cortical F-actin lost its smooth distribution and was drastically fragmented (Fig. 9A). A further difference between the phenocopy and the mutants is that restoration of a smooth cortical F-actin layer after its nuclear penetration never occurred in phenocopies (Fig. 9B). Cortical nuclei in cytochalasin-treated embryos frequently showed irregular distribution, resulting from collisions between adjacent nuclei after their divisions (Fig. 9C). This confirmed the report by Zalokar and Erk (1976). In addition, the cellularization of blastoderm was inhibited in the phenocopies.

Cytological mapping of N26 and N441

Cytological map positions of *N26* and *N441* were determined by crossing mutant males with strains with deficiencies covering their respective loci on the X-chromosome. *N26* was complemented by *Df(1)ras-v-Cc8*, *Df(1)N71* and *Df(1)HA85* but not by *Df(1)RA37*. *N441* was complemented by *Df(1)KA6*, *Df(1)KA10* and *Df(1)C246* but not by *Df(1)N105*, *Df(1)JA26* and *Df(1)HF368*. From these results, cytological map positions of *N26* and *N441* were located at 10A6-B3 and 11A7-B9, respectively. These loci do not coincide with any reported genetic loci of cytoskeletal proteins. *par* has been located at 3B3 (Thierry-Mieg, 1982), at which no cytoskeletal protein gene is known to be located either.

Hemizygous phenotypes of mutants

Embryos derived from *N441/Df(1)N105* females were completely identical in the phenotype to ones derived from *N441/N441* females. On the other hand, embryos derived from *Df(1)N105/+* and *N441/+* females showed a complete wild-type phenotype. Thus the *N441* mutation probably behaves as an amorphic allele under a restrictive condition.

About a half (32 out of 62) of the embryos derived from *Df(1)RA37/+* females terminated their development at an early cleavage stage. This is probably due to the lack of the *hfs* locus in *Df(1)RA37*, which has been reported to cause haplo-insufficient female sterility (Lefevre, 1969; Zhimulev *et al.* 1981; Eberl and Hilliker, 1988). *N26* complemented hfs^{EH326}. Embryos that derived from *Df(1)RA37/+* females and survived early cleavage stage skipped egg contraction (79%, 11 out of 14) and showed slight retardation in nuclear migration and in the transition of the central domain of F-actin to the energid domain. The central domain was observed, in some cases, as late as at cycle 6. On the other hand, in 86% (69 out of 80) of embryos derived from *N26/Df(1)RA37* females, development was arrested at an early cleavage stage or before the first cleavage. The nuclear migration and the transition of F-actin distribution in these embryos were similar to those in embryos derived from *N26/N26* females. Affected by extreme regional differences in the timing of blastodermal cellularization along the anteroposterior axis, embryos derived from *N26/Df(1)RA37* females showed strong disorder in morphogenesis even if they had wild-type fathers, and rarely hatched out. Embryos derived from *N26/+* females could not be distinguished from wild-type embryos. Thus *N26* is regarded as a hypomorphic mutation of a gene causing haplo-insufficient female sterility, and is independent of *hfs* although located in the 10A–B region. Embryos derived from $par/Df(1)w^{258\text{-}45}$ females were principally the same as those derived from *par/par* females concerning nuclear migration and the distribution of F-actin. None of the three mutations that we examined showed detectable zygotic lethality in hemizygous females.

Discussion

Possible wild-type function of the mutant genes

Here we showed in *Drosophila* that the three X-linked maternal-effect mutations caused a similar disorder in F-actin reorganization in cleavage embryos. It was verified that the cytological loci of *N26* and *N441* are separated from any of the six reported actin loci (Tobin

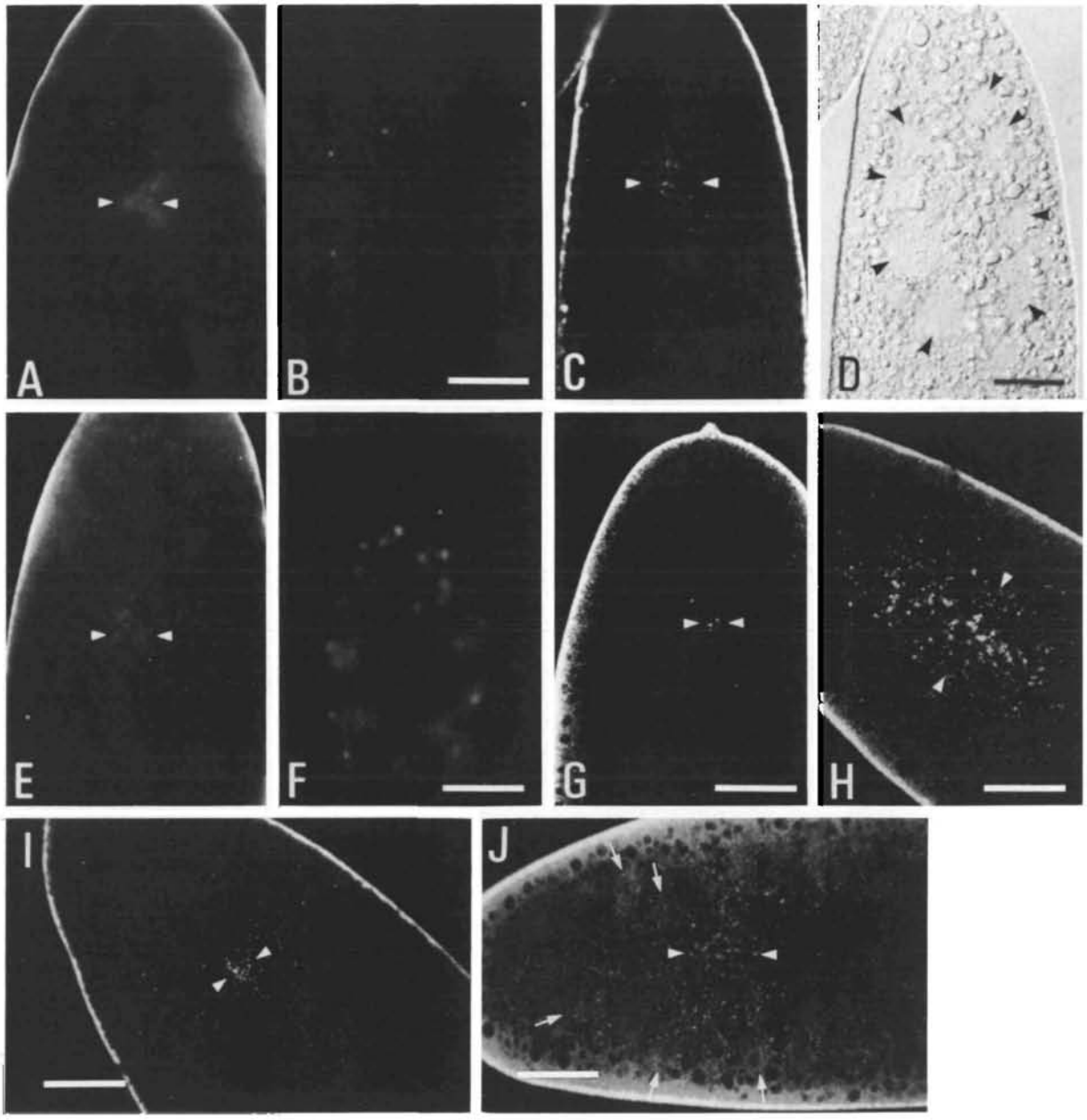

Fig. 8. F-actin distribution in mutant embryos. Embryos were stained with rhodaminyl phalloidin in A, C, E and G–J; with DAPI in B and F. (D) An interference contrast image of the same embryo shown in C to visualize energids (arrowheads). (A and G) Cycle-6 *N441* embryos; (C, H and J) *N26* embryos at cycle 6, 8 and 9 respectively; (E and I) *par* embryos at cycle 7. (A and B), (C and D), and (E and F) are the combinations of the same double-stained embryos photographed with different excitation light, respectively. (A), (B), (E) and (F) Anterior part of whole-mount embryos; (C and D) the same frozen section observed with different optics; (G–J) confocal images of the anterior part of whole-mount embryos. The central domain of F-actin is shown between arrowheads in (A, C, E, and G–I). In the embryo shown in J, transition of F-actin distribution from the central (between arrowheads) to the energids (arrows) is in progress. Anterior poles are to the top in A–G, to the top-left corner in H and I, and to the left in J. Bars represent 50 μm.

et al. 1980; Fyrberg *et al.* 1980) and also from the so-far known genetic loci of other cytoskeletal proteins (see Fyrberg, 1989 for review). The cytological locus of *par* has been located at 3B3 (Thierry-Mieg, 1982), at which no cytoskeletal protein has been mapped. In addition, homozygous *N26* and *N441* were comparable to wild-type strains in the relative amount of actin in an ovarian egg and in a deriving embryo, as revealed with two-dimensional gel electrophoresis (Hatanaka, unpublished). Thus the abnormal F-actin reorganization in *N26* and *N441* embryos cannot be ascribed to abnormal structure or inadequate amount of actin molecules, but presumably to molecules other than actin.

The cortical F-actin layer, which is smooth in wild type, is rough in mutant embryos due to aggregates scattered over its inner surface. However, the layer is

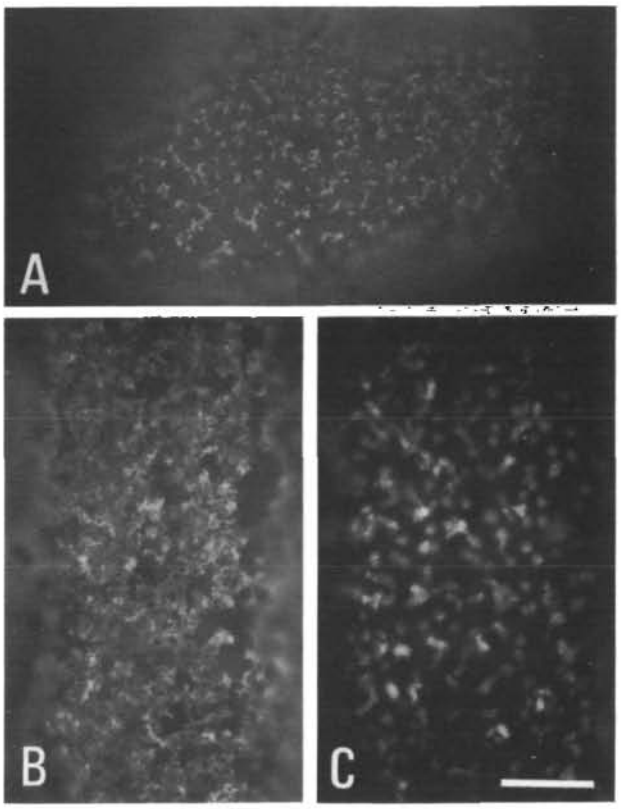

Fig. 9. Fragmented cortical F-actin layer of wild-type embryos treated with 1 $\mu g\,ml^{-1}$ cytochalasin B for 5 min. (A) A cycle-7 embryo treated with cytochalasin B at cycle 2 and (B) a syncytial blastoderm embryo treated with cytochalasin B at cycle 8. (C) the same field shown in B, but nuclei are visualized by DAPI staining. Focus is on the surface of whole-mount embryos. Bar represents 50 μm.

not fragmented as it is in the cytochalasin-induced phenocopy. Such a rough surfaced F-actin layer was never induced by cytochalasins under any conditions that we examined. These results suggest that the abnormal reorganization of cortical F-actin caused by these mutations does not result from simple disruption of polymerization. At this moment, it is rather premature to draw a conclusion, but we are inclined to presume that a wild-type function of the genes in this study is essential for reorganization of cortical F-actin triggered to be initiated at fertilization, and this reorganization enables embryos to contract and is probably essential for normal nuclear migration (see below).

F-actin reorganization is required for cleavage nuclei to migrate and penetrate periplasm simultaneously

The developmental changes of distribution pattern of F-actin and nuclei in wild-type and mutant embryos at three stages were highly reproducible in the present study, and are schematically summarized in Fig. 10. In many insect groups, nuclei are distributed more or less spherically within the yolk mass in embryos at the mid-cleavage stage (Counce, 1973). In *Drosophila*, this type of nuclear distribution is distinct only during cycle 2 through 4 (Zalokar and Erk, 1976; the present observation), and this is the very period when the central domain of F-actin is present (Fig. 10A). At cycle

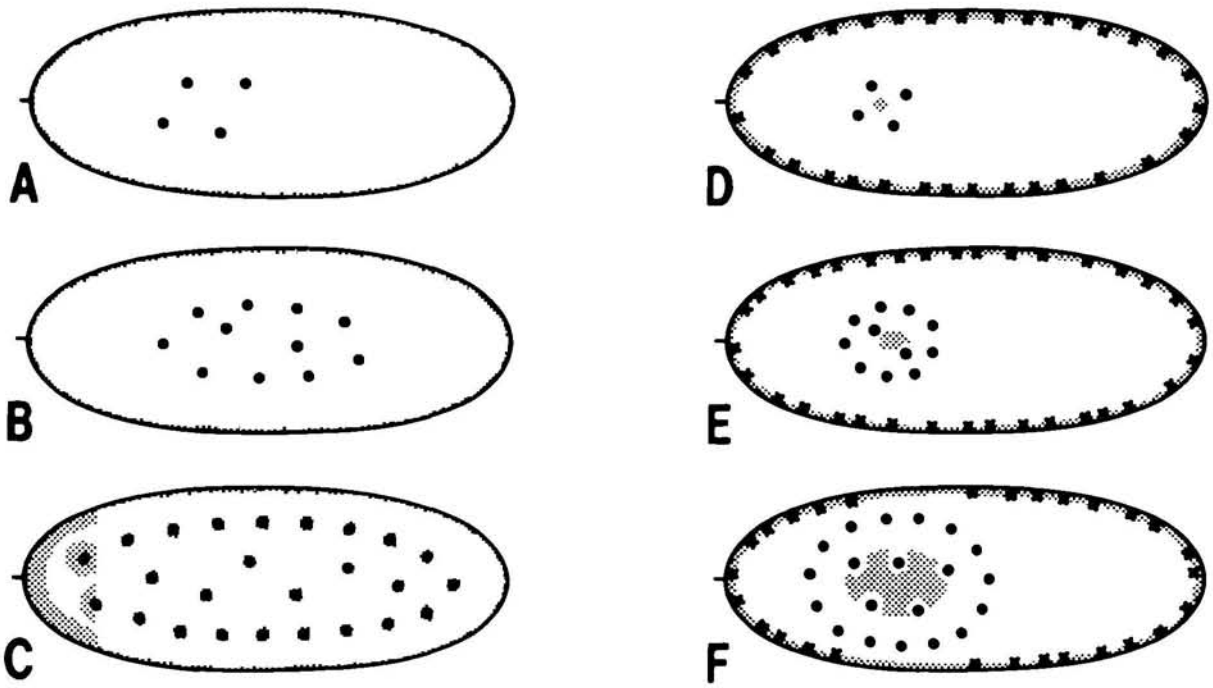

Fig. 10. Schematic representation of the develolpmental changes in the distributions of nuclei and F-actin in wild-type (A–C) and mutant (D–F) embryos. Cycle-3 (A and D), cycle-5 (B and E) and cycle-7 (C and F) embryos are shown. Filled circles represent nuclei, shaded areas represent the regions where F-actin is detectable and crosses represent mutant-type F-actin aggregates in the cortex.

5, the spatial distribution pattern of nuclei has already been elongated anteroposteriorly (Zalokar and Erk, 1976; the present observation). This change in distribution of nuclei accompanies the transition of F-actin distribution from the central to the energid domain (Fig. 10B). Afterwards, gradually approaching the cortex, nuclei are distributed equidistantly from the cortex as well as from each other (Fig. 10C). On the other hand, both in the mutants and in the phenocopies, their retarded nuclear migration toward the poles was always accompanied by a delay in the development of the central domain of F-actin and its transition to the energid domain (Fig. 10D–F). These results suggest that F-actin in the inner cytoplasm is involved in the mechanism of nuclear migration in *Drosophila* cleavage embryos.

In the mutant and phenocopied embryos, nuclei remain in the anterior region retaining their spherical distribution for much longer period of time than in the wild type. The sphere carrying nuclei keeps growing to contact the cortex where premature nuclear penetration occurs. In contrast, in the wild type, nuclei are inhibited from reaching the cortex before cycle 10 except in the posterior pole region. In addition, the distance between neighboring nuclei is shorter in the mutants than in the wild type. Probably the function of the wild-type F-actin organization is necessary to keep each nucleus apart from its neighbors and also from the cortex during the cleavage stages. Although we have obtained no clue to explain how F-actin organization works in cleavage embryos, it may, by itself or in collaboration with other cytoskeletal elements, stiffen the cytoplasm enough to act as a mechanical barrier. Our assumption is that there is a genetical regulation to maintain this barrier through the cleavage stage and then to make it abruptly disappear to ensure simultaneous nuclear penetration of periplasm in the somatic region. Our results from colchicine treatment of embryos suggest that microtubules are responsible for giving nuclei the final thrust to enter into the periplasm.

Comparison with other insects

It has been reported that cytochalasin B does not inhibit the nuclear migration in the cleavage embryo of a gall midge *Wachtliella* (Wolf, 1978). Although the cause of the discrepancy between the gall midge and *Drosophila* is unknown, the following explanation is possible. In *Drosophila*, F-actin keeps cleavage nuclei a certain distance away from the periplasm during the cleavage stage, and this causes the initial spherical distribution of nuclei to change into the final elongated ellipsoid distribution lining the periplasm. In *Wachtliella*, however, the egg is extremely elongated, and has only space for energids in a single file in the early cleavage stage (Wolf, 1969), and so the embryo does not have any stage when nuclei are distributed spherically as in *Drosophila*. Thus it is probable that an F-actin-dependent nuclear migration mechanism has not developed or has secondarily disappeared in *Wachtliella*. In many insect species, nuclei penetrate the periplasm almost synchronously in all egg regions in spite of the initial spherical nuclear distribution and the varieties in egg shapes. Thus we presume that a gene like $N441^+$ is conserved in various insect species to function during the cleavage stage.

Genetical analysis

Our genetic analysis showed that both *N441* and *par* are amorphic under the restrictive condition that we used, although it has been reported that *par* behaves like an antimorphic allele (Thierry-Mieg, 1982). In addition to the maternal effects that we described, *N26* and *par* have a zygotic effect. Both *N26*/Y and *par*/Y male flies showed a low lethality at the pupal stage. Moreover, all five strains with the double mutation of *N26* and *par* showed a high recessive zygotic lethality at the pupal stage regardless of sex (Hatanaka, unpublished data). This high lethality cannot be explained as a simple additional effect of the mutations, since there was no detectable lethality in *N26/N26*, *N26/Df(1)RA37*, *par/par* and $par/Df(1)w^{258\text{-}45}$ females. It is still unknown whether their pupal lethality is caused by defective F-actin reorganization or not, *N26* and *par* may have some defects in a closely related mechanism operating in pupal development. Among the three mutants that we tested, only *N441* behaved as a simple recessive maternal-effect mutant. Thus we are inclined to regard $N441^+$ as a candidate for a gene that has a key role in a mechanism underlying cleavage-stage-specific F-actin reorganization.

We thank Dr M. Masson for providing *par* stocks, Dr D. Thierry-Mieg for the information about the *par* phenotype, Dr D. F. Eberl for providing *hfs* stock, and Dr T. Ode for discussion. We also thank Dr M. Katori (Kitasato University) for allowing K.H. to use his laboratory equipments for the preparation of the manuscript. This work was supported in part by a Grant-in-Aid from the Ministry of Education, Science and Culture, Japan.

References

Counce, S. J. (1973). The causal analysis of insect embryogenesis. In *Developmental Systems: Insects*, vol. 2 (ed. S. J. Counce and C. H. Waddington), pp. 1–156. New York: Academic Press.

Eberl, D. F. and Hilliker, A. J. (1988). Characterization of X-linked recessive lethal mutations affecting embryonic morphogenesis in *Drosophila melanogaster*. *Genetics* **118**, 109–120.

Foe, V. E. and Alberts, B. M. (1983). Studies of nuclear and cytoplasmic behaviour during the five mitotic cycles that precede gastrulation in *Drosophila* embryogenesis. *J. Cell Sci.* **61**, 31–70.

Freeman, M., Nüsslein-Volhard, C. and Glover, D. M. (1986). The dissociation of nuclear and centrosomal division in *gnu*, a mutation causing giant nuclei in *Drosophila*. *Cell* **46**, 457–468.

Fyrberg, E. (1989). Study of contractile and cytoskeletal proteins using *Drosophila* genetics. *Cell Motility and the Cytoskeleton* **14**, 118–127.

Fyrberg, E. A., Kindle, K. L. and Davidson, N. (1980). The actin genes of *Drosophila*: a dispersed multigene family. *Cell* **19**, 365–378.

Gans, M., Audit, C. and Masson, M. (1975). Isolation and characterization of sex-linked female-sterile mutants in *Drosophila melanogaster*. *Genetics* **81**, 683–704.

Karr, T. L. and Alberts, B. M. (1986). Organization of the cytoskeleton in ealry *Drosophila* embryos. *J. Cell Biol.* **102**, 1494–1509.

LEFEVRE, G., JR (1969). The eccentricity of vermilion deficiencies in *Drosophila melanogaster*. *Genetics* **63**, 589–600.

LIMBOURG, B. AND ZALOKAR, M. (1973). Permeabilization of *Drosophila* eggs. *Devl Biol.* **35**, 382–387.

LINDSLEY, D. AND ZIMM, G. (1987). The genome of *Drosophila melanogaster*, part 3: rearrangements (ed. P. W. Hedrick). *Drosophila Information Service* **65**.

MARUO, F. AND OKADA, M. (1984). Functions of a maternal gene are required for the synchronous nuclear division during early development of *Drosophila melanogaster*. Analyses on a ts-mutant. *Zool. Sci.* **1**, 405–414.

MERRILL, P. T., SWEETON, D. AND WEISCHAUS, E. (1988). Requirements for autosomal gene activity during precellular stages of *Drosophila melanogaster*. *Development* **104**, 495–509.

MILLER, K. G., KARR, T. L., KELLOGG, D. R., MOHR, I. J., WALTER, M. AND ALBERTS, B. M. (1985). Studies on the cytoplasmic organization of early *Drosophila* embryos. In *Molecular Biology of Development. Cold Spring Harbor Symposia on Quantitative Biology*, vol. 50, pp. 79–90. New York: Cold Spring Harbor Laboratory.

MOHLER, J. D. (1977). Developmental genetics of the *Drosophila* egg. I. Identification of 59 sex-linked cistrons with maternal effects on embryonic development. *Genetics* **85**, 259–272.

NIKI, Y. (1984). Developmental analysis of the *grandchildless (gs(1)N26)* mutation in *Drosophila melanogaster*: Abnormal cleavage patterns and defects in pole cell formation. *Devl Biol.* **103**, 182–189.

NIKI, Y. AND OKADA, M. (1981). Isolation and characterization of *grandchildless*-like mutants in *Drosophila melanogaster*. *Wilhelm Roux's Arch. devl Biol.* **190**, 1–10.

OKADA, M. (1982). Loss of the ability to form pole cells in *Drosophila* embryos with artificially delayed nuclear arrival at the posterior pole. In *Embryonic Development Pt.A:Genetic Aspects* (ed. by M. M. Burger and G. Weber), pp. 363–372. New York: Alan R. Liss.

THIERRY-MIEG, D. (1976). Study of a temperature-sensitive mutant grandchildless-like in *Drosophila melanogaster*. *J. Microsc. Biol. Cell.* **25**, 1–6.

THIERRY-MIEG, D. (1982). Paralog, a control mutant in *Drosophila melanogaster*. *Genetics* **100**, 209–237.

TOBIN, S. L., ZULAUF, E., SANCHEZ, F., CRAIG, E. A. AND MCCARTHY, B. J. (1980). Multiple actin-related sequences in the *Drosophila melanogaster* genome. *Cell* **19**, 121–131.

WARN, R. M. AND MAGRATH, R. (1983). F-actin distribution during the cellularization of the *Drosophila* embryo visualized with FL-phalloidin. *Expl Cell Res.* **143**, 103–114.

WARN, R. M., MAGRATH, R. AND WEBB, S. (1984). Distribution of F-actin during cleavage of the *Drosophila* syncytial blastoderm. *J. Cell Biol.* **98**, 156–162.

WARN, R. M., SMITH, L. AND WARN, A. (1985). Three distinct distributions of F-actin occur during the divisions of polar surface caps to produce pole cells in *Drosophila* embryos. *J. Cell Biol.* **100**, 1010–1015.

WARN, R. M. AND WARN, A. (1986). Microtubule arrays present during the syncytial and cellular blastoderm stage of the early *Drosophila* embryo. *Expl Cell Res.* **163**, 201–210.

WARN, R. M. (1986). The cytoskeleton of the early *Drosophila* embryo. *J. Cell Sci. Suppl.* **5**, 311–328.

WIESCHAUS, E. AND SWEETON, D. (1988). Requirements for X-linked zygotic gene activity during cellularization of early *Drosophila* embryos. *Development* **104**, 483–493.

WOLF, R. (1969). Kinematik und Feinstruktur plasmatischer Faktorenbereiche des Eies von *Wachtliella persicariae* L. (Diptera). I. Das Verhalten ooplasmatischer Teilsysteme im normalen Ei. *Wilhelm Roux's Arch. EntwMech. Org.* **162**, 121–160.

WOLF, R. (1978). The cytaster, a colchicine-sensitive migration organelle of cleavage nuclei in an insect egg. *Devl Biol.* **62**, 464–472.

ZALOKAR, M., AUDIT, C. AND ERK, I. (1975). Developmental defects of female-sterile mutants of *Drosophila melanogaster*. *Devl Biol.* **47**, 419–432.

ZALOKAR, M. AND ERK, I. (1976). Division and migration of nuclei during early embryogenesis of *Drosophila melanogaster*. *J. Microsc. Biol. Cell.* **25**, 97–106.

ZALOKAR, M. AND ERK, I. (1977). Phase-partition fixation and staining of *Drosophila* eggs. *Stain Technol.* **52**, 89–95.

ZHIMULEV, I. F., POKHOLKOVA, G. V., BGATOV, A. V., SEMESHIN, V. F. AND BELYAEVA, E. S. (1981). Fine cytogenetical analysis of the band 10A1-2 and the adjoining regions in the *Drosophila melanogaster* X chromosome. II. Genetical analysis. *Chromosoma* **82**, 25–40.

(*Accepted 20 December 1990*)